The Eurasia Proceedings of Science, Technology, Engineering & Mathematics (EPSTEM)
ISSN: 2602-3199

The Eurasia Proceedings of Science, Technology, Engineering & Mathematics (EPSTEM), 2023

Volume 23, Pages 143-150

ICRETS 2023: International Conference on Research in Engineering, Technology and Science

Non-linear Viscoelastic Beams Under Periodic Strains: An Approach for Analyzing of Longitudinal Fracture

Victor Rizov
University of Architecture, Civil Engineering and Geodesy

Abstract: This work describes a longitudinal fracture analysis of beam structure of circular cross-section under periodic strains. The material whose properties vary in radial direction has non-linear viscoelastic behaviour. The beam is loaded in torsion so that the twist angle represents a periodical function. Time-dependent behaviour under periodic strains is dealt with a model having a non-linear spring and a linear dashpot. The complementary strain energy in the beam is considered to determine the strain energy release rate. The balance of energy is examined to verify the strain energy release rate. The ascendency of various parameters over strain energy release rate is assessed.

Keywords: Non-linear viscoelastic beam, Longitudinal fracture, Periodic strain

Introduction

One of the important tasks of up-to-date material science is the development and perfecting of continuously inhomogeneous structural materials. The properties of these materials are contingent on coordinates. In recent decades, the functionally graded materials have emerged as an advanced type of materials with continuous inhomogeneity (Fanani et al., 2021; Mahamood & Akinlabi, 2017; Nikbakht et al., 2019; Oza et al., 2021). The change of microstructure of functionally graded materials in a structural member or component is formed in a desired way during manufacturing (Dias et al., 2010; Gururaja Udupa et al., 2014; Gandra et al., 2011; Radhika et al., 2020).

In their life-time, many engineering structures made of continuously inhomogeneous materials undergo non-linear viscoelastic deformation under periodic loading that must be considered when analyzing fracture. On account of that, the aim of this work is to examine in analytical way the longitudinal fracture of a non-linear viscoelastic beam under periodic strains (prior papers in this field are focussed on linear viscoelastic beams (Narisawa, 1987; Rizov, 2022; Rizov, 2022). The beam under examination has a circular section and is inhomogeneous in radial direction. The beam is under torsion. The strain energy release rate (SERR) is determined. The balance of energy (BE) is considered for control of the SERR solution.

Theoretical Analysis

In this paper, the non-linear viscoelastic mechanical model in Fig. 1 is used. The model consists of a non-linear spring with shear modulus, G_f, placed in parallel to a dashpot of linear behaviour (the viscosity coefficient is η). Shear strain, γ, in the model is a periodical function of time, t, as depicted in Fig. 2. The period of the shear strains is T. The maximum value of shear strains is γ_m. The period of shear strains is presented as $T = T_b + T_d$ where $T_b = pT$, $0 < p < 1$ (Fig. 2). Thus, $T_d = (1 - p)T$.

- Selection and peer-review under responsibility of the Organizing Committee of the Conference

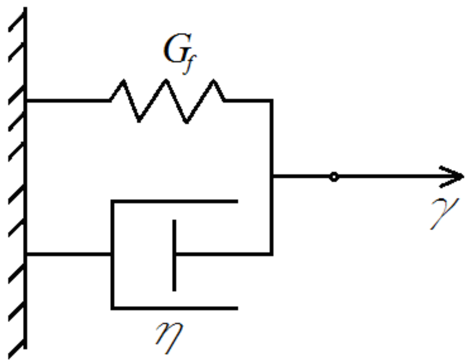

Figure 1. Non-linear viscoelastic model.

The shear strain is expanded in series of Fourier

$$\gamma(t) = q_0 + \sum_{j=1}^{\infty} q_j \cos(j\overline{\omega}t) + \sum_{j=1}^{\infty} r_j \sin(j\overline{\omega}t),\ \ \overline{\omega} = \frac{2\pi}{T}. \tag{1}$$

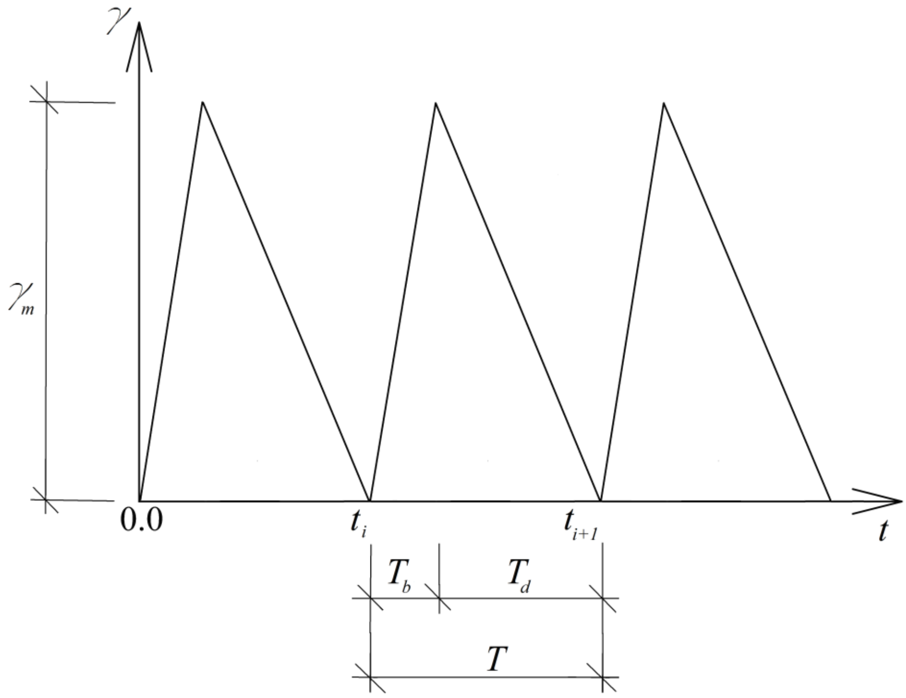

Figure 2. Periodic change of the shear strain.

by using the formulae

$$q_0 = \frac{1}{T}\int_0^T \gamma dt,\ \ q_j = \frac{2}{T}\int_0^T \gamma \cos(j\overline{\omega}t)dt,\ \ r_j = \frac{2}{T}\int_0^T \gamma \sin(j\overline{\omega}t)dt, \tag{2}$$

the coefficients in (1) are found as

$$q_0 = \frac{\gamma_m}{2},\ \ q_j = \frac{2\gamma_m}{T^2}\left\{\ \frac{1}{pj^2\overline{\omega}^2}\left[j\overline{\omega}pT\sin(j\overline{\omega}pT) + \cos(j\overline{\omega}pT) - 1\right] + \right.$$

$$+\frac{T}{(1-p)\,j\varpi}\left[\sin\left(j\varpi T\right)-\sin\left(j\varpi pT\right)\right]-$$

$$-\frac{1}{(1-p)\,j^2\varpi^2}\left[\ Tj\varpi\sin\left(j\varpi T\right)+\cos\left(j\varpi T\right)-pTj\varpi\sin\left(j\varpi pT\right)-\cos\left(j\varpi pT\right)\ \right]\Bigg\},\tag{3}$$

$$r_j=\frac{2\gamma_m}{T^2}\Bigg\{\ \frac{1}{pj^2\varpi^2}\left[\ \sin\left(j\varpi pT\right)-j\varpi Tp\cos\left(j\varpi pT\right)\ \right]+$$

$$+\frac{T}{(1-p)j\varpi}\Bigg\{\left[\ \cos\left(j\varpi pT\right)-\cos\left(j\varpi T\right)\ \right]-$$

$$-\frac{1}{(1-p)j^2\varpi^2}\left[\ \sin\left(j\varpi T\right)-j\varpi T\cos\left(j\varpi T\right)-\sin\left(j\varpi pT\right)+j\varpi pT\cos\left(j\varpi pT\right)\ \right]\Bigg\}.\tag{4}$$

0

The shear stress, τ_f, in the spring and the shear stress, τ_η, in the linear dashpot (Fig. 1) are expressed by the following laws:

$$\tau_f=G_f\gamma^n\,,\ \tau_\eta=\eta\dot{\gamma}\,,\tag{5}$$

where n is a material property, η is the coefficient of viscosity.

The shear stress (refer to Fig. 1) is deduced as

$$\tau=\tau_f+\tau_\eta\,.\tag{6}$$

By using (1), (5) and (6), one derives

$$\tau=G_f\left[\ q_0+\sum_{j=1}^{\infty}q_j\cos\left(j\varpi t\right)+\sum_{j=1}^{\infty}r_j\sin\left(j\varpi t\right)\ \right]^n+$$

$$+\eta\left[\ \sum_{j=1}^{\infty}-q_j\,j\varpi\sin\left(j\varpi t\right)+\sum_{j=1}^{\infty}r_j\,j\varpi\cos\left(j\varpi t\right)\ \right].\tag{7}$$

By combining of (5) and (7), one obtains

$$\tau=G_f\gamma^n+\eta\left[\ \sum_{j=1}^{\infty}-q_j\,j\varpi\sin\left(j\varpi t\right)+\sum_{j=1}^{\infty}r_j\,j\varpi\cos\left(j\varpi t\right)\ \right].\tag{8}$$

Dependence (8) represents the non-linear stress-strain-time law of model (Fig. 2).

This law is used to model the mechanical behaviour of the clamped structure sketched in Fig. 3. The beam cross-section is a circle of radius, R_1. The beam longitudinal size is l. We are focussed on a longitudinal crack in the form of cylindrical surface of radius, R_2. The crack longitudinal size is a as depicted in Fig. 3. The beam is under torque so that the twist angle, φ, of external crack arm (the external crack arm section has internal and external radius, R_2 and R_1, respectively) changes periodically with time (at $t_i \le t \le t_i + T_b$ the angle of twist grows from 0 to φ_h ; at $t_i + T_b \le t \le t_i + T$ the angle decreases from φ_h to 0). The internal arm of crack is unstressed (the internal arm of crack has circular section with radius, R_2).

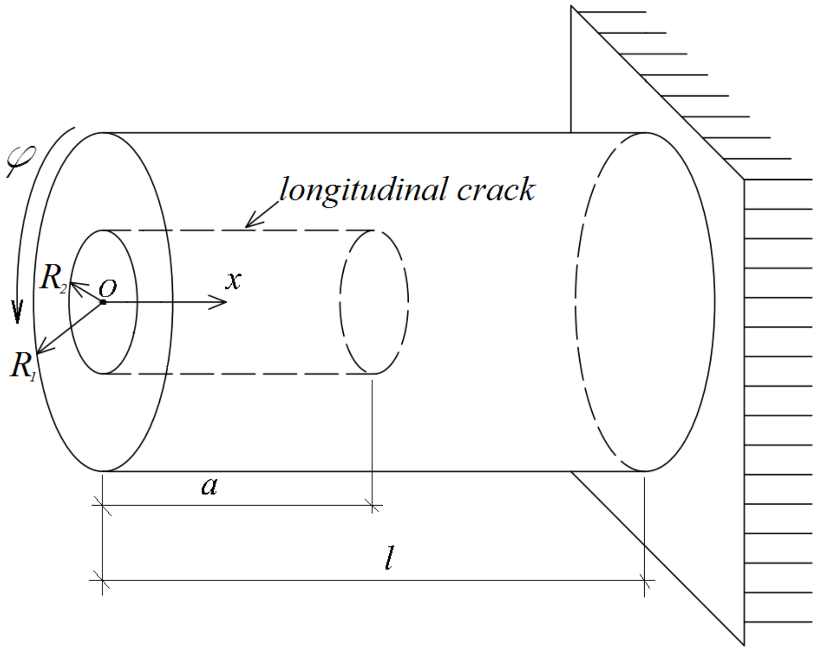

Figure 3. Static scheme of beam under examination.

The beam is inhomogenous in radial direction. Thus, material properties, G_f and η, change exponentially along section radius

$$G_f = G_{f0} e^{s\frac{R}{R_1}}, \; \eta = \eta_0 e^{g\frac{R}{R_1}}. \tag{9}$$

Here, G_{f0} and η_0 are G_f and η magnitudes in the section centre, s and g are parameters.

The SERR, G , for the longitudinal crack (Fig. 3) is deduced as

$$G = \frac{dU^*}{2\pi R_2 da}, \tag{10}$$

where the complementary strain energy (CSE) in the beam is

$$U^* = U_1^* + U_2^* = a\int_{R_2}^{R_1} u_{01}^* 2\pi R dR + (l-a)\int_0^{R_1} u_{02}^* 2\pi R dR. \tag{11}$$

Here, u_{01}^* and u_{02}^* are CSE densities in the external arm of crack and in the intact portion of beam. u_{01}^* is calculated as

$$u_{01}^* = \tau\gamma - \int_0^{\gamma} \tau d\gamma . \tag{12}$$

The shear strain in section of the external arm of crack is

$$\gamma = \frac{\gamma_{ek}}{R_1} R \, . \tag{13}$$

In dependence (13), γ_{ek} is the strain magnitude at the surface.

The CSE density in the intact portion of beam is found by substituting $\tau = \tau_{un}$ and $\gamma = \gamma_{un}$ in formula (12) (τ_{un} and γ_{un} the shear stress and shear strain in the intact portion of beam). Distribution of γ_{un} in section of the intact portion of beam is obtained by substituting of $\gamma_{ek} = \gamma_{hw}$ in (13). Here, γ_{hw} is the strain magnitude at the surface of the intact portion of beam.

γ_{ek} and γ_{hw} are determined by applying the following approach. First, two equilibrium equations are formulated

$$T = \int_{R_2}^{R_1} \tau 2\pi R^2 dR \, , \; T = \int_{0}^{R_1} \tau_{un} 2\pi R^2 dR \, . \tag{14}$$

where T is the torque in the external arm of crack.

Further, it follows from the Maxwell-Mohr integrals that

$$\varphi = \frac{\gamma_{ek}}{R_1} a + \frac{\gamma_{hw}}{R_1} \left(l - a \right). \tag{15}$$

γ_{ek} , γ_{hw} and T are determined from (14) and (15) by MatLab.

After combining of (10) and (11), one derives

$$G = \frac{1}{R_2} \left(\int_{R_2}^{R_1} u_{01}^{*} R dR - \int_{0}^{R_1} u_{02}^{*} R dR \right). \tag{16}$$

Integrals in (16) are treated by MatLab.

In order to verify (16), the SERR is determined as well by analyzing the BE. The result is

$$G = \frac{T}{2\pi R_2} \frac{\partial \varphi}{\partial a} - \frac{1}{2\pi R_2} \frac{\partial U}{\partial a} \, . \tag{17}$$

Here, the strain energy (SE), U , is reckoned by using (11) and (12). For this purpose, the CSE densities are replaced with the SE densities, u_{01} and u_{02} . The SE density in the external arm of crack is

$$u_{01} = \int_{0}^{\gamma} \tau d\gamma \, . \tag{18}$$

The SE density in the intact portion of beam is calculated by replacing of τ with τ_{un} in (18). By substituting of φ and U in (17), one obtains

$$G = \frac{T}{2\pi R_2}\left(\frac{\gamma_{ek}}{R_1} - \frac{\gamma_{hw}}{R_1}\right) - \frac{1}{R_2}\int_{R_2}^{R_1} u_{01} R dR + \frac{1}{R_2}\int_{0}^{R_1} u_{02} R dR. \quad (19)$$

Integrals in (19) are treated by MatLab. The SERR reckoned by (19) and (16) are match which is a verification of the present analysis.

Numerical Results

The SERR calculations are carried-out by using the following data: $R_1 = 0.008$ m, $l = 0.300$ m, $n = 0.6$, $p = 0.5$, $T = 80$ sec and $\varphi_h = 0.001$ rad.

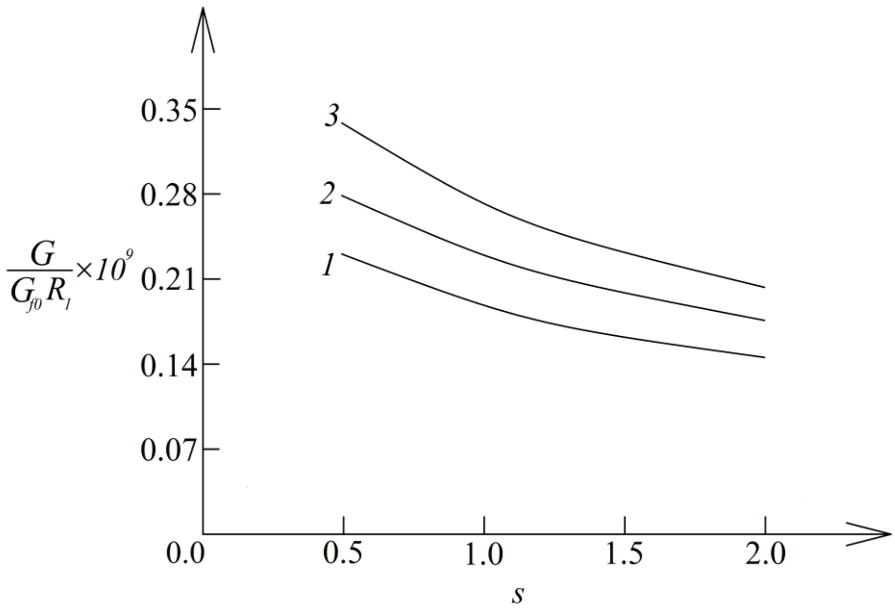

Figure 4. SERR - s curves (1 – at $R_2 / R_1 = 0.4$, 2 – at $R_2 / R_1 = 0.6$ and 3 – at $R_2 / R_1 = 0.8$).

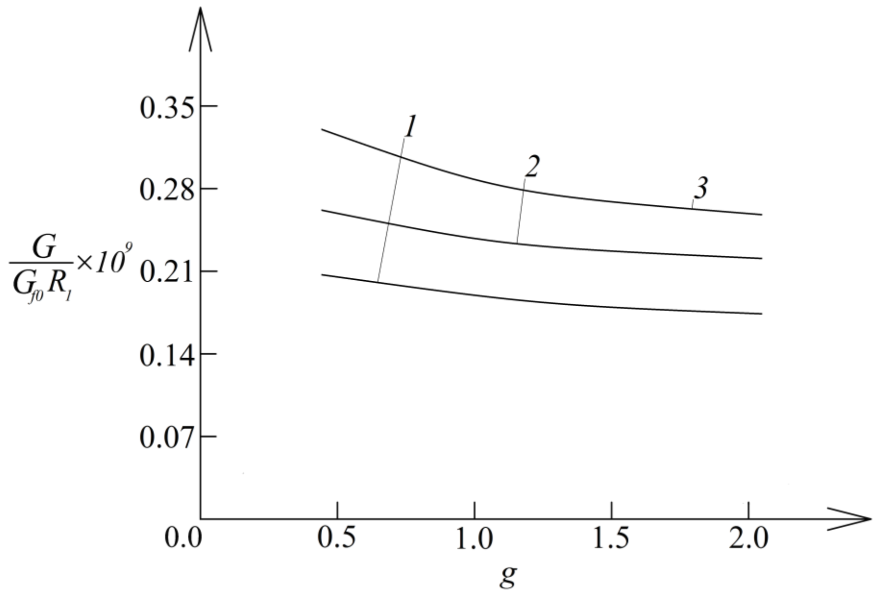

Figure 5. SERR - g curves (1 - at $\varphi_h = 0.0006$ rad, 2 - at $\varphi_h = 0.0008$ rad and 3 - at $\varphi_h = 0.001$ rad).

The SERR - s curves are presented at three R_2 / R_1 ratios in Fig. 4. The curves in Fig. 4 indicate that SERR reduces when s grows. However, growth of R_2 / R_1 ratio generates growth of SERR (Fig. 4). The influence of φ_h and g on SERR is assessed (Fig. 5). When the twist angle, φ_h, increases, SERR also increases. Increase of parameter, g, reduces SERR (Fig. 5).

Conclusion

An approach for analytical examination of the longitudinal fracture in non-linear viscoelastic inhomogeneous beam structure under periodically changing strains is presented. The beam is subjected to pure torsion. A model of non-linear spring placed in parallel to a linear dashpot is used for describing the beam mechanical behaviour. A solution of SERR that accounts for the beam non-linear viscoelastic deformation under periodic loading is derived. The influence of the periodic loading on SERR is assessed. Reckons of SERR are carried-out at different magnitudes of twist angle, φ_h. It is found that growth of φ_h generates growth of SERR. The SERR increases as well with growth of R_2 / R_1 ratio. The growth of parameters, s and g, induces reduction of SERR.

Recommendations

The approach presented in this paper can be developed further by analyzing the longitudinal fracture of beams subjected to torsion and bending under periodic strains.

Scientific Ethics Declaration

The author declares that the scientific ethical and legal responsibility of this article published in EPSTEM journal belongs to the author.

Acknowledgements or Notes

* This article was presented as a poster presentation at the International Conference on Research in Engineering, Technology and Science (www.icrets.net) held in Budapest/Hungary on July 06-09, 2023.

References

Dias, C. M. R., Savastano, Jr. H., & John, V. M. (2010). Exploring the potential of functionally graded materials concept for the development of fiber cement. *Construction and Building Materials, 24,* 140-146.

Fanani, E.W.A., Surojo, E., Prabowo, A. R., & Akbar, H. I. (2021). Recent progress in hybrid aluminum composite: Manufacturing and application. *Metals, 11,* 1919-1929.

Gandra, J., Miranda, R., Vilaca, P., Velhinho, A., & Teixeira, J.P. (2011). Functionally graded materials produced by friction stir processing. *Journal of Materials Processing Technology, 211,* 1659-1668.

Gururaja U., Shrikantha Rao S., & Rao Gangadharan, K. (2014). Functionally graded composite materials: An overview. *Procedia Materals Science, 5,* 1291-1299.

Mahamood, R. C., & Akinlabi, E. T. (2017). *Functionally graded materials.* Springer.

Nikbakht, S., Kamarian, S., & Shakeri, M. (2019). A review on optimization of composite structures Part II: Functionally graded materials. *Composite Structures, 214,* 83-102.

Narisawa, I. (1987). Strength of polymer materials. *Chemistry,* 400.

Oza, M. J., Schell, K. G., Bucharsky, E. C., Laha, T., & Roy, S. (2021). Developing a hybrid Al–SiC-graphite functionally graded composite material for optimum composition and mechanical properties. *Materials Science and Engineering: A, 805,* 140625.

Radhika, N., Sasikumar, J., Sylesh, J. L., & Kishore, R. (2020). Dry reciprocating wear and frictional behaviour of B4C reinforced functionally graded and homogenous aluminium matrix composites. *Journal of Materials Research and Technology, 9,* 1578-1592.

Rizov, V.I. (2022). Effects of periodic loading on longitudinal fracture in viscoelastic functionally graded beam structures. *J. Appl. Comput. Mech*., *8,* 370–378.

Rizov, V.I. (2022). Viscoelastic inhomogeneous beam subjected to mechanical loading and periodically varying temperature: a longitudinal fracture analysis. *Procedia Structural Integrity 41*, 103–114.

Author Information

Victor Rizov
University of Architecture, Civil Engineering and Geodesy
Sofia, Bulgaria
Contact e-mail: *v_rizov_fhe@uacg.bg*

To cite this article:

Rizov, V. (2023). Non-linear viscoelastic beams under periodic strains: An approach for analyzing of longitudinal fracture. *The Eurasia Proceedings of Science, Technology, Engineering & Mathematics (EPSTEM)*, *23*, 143-150.